MODELING THE INFLUENCE OF CRACK PATH DEVIATIONS ON THE PROPAGATION OF STRESS CORROSION CRACKS

Richard E. Ricker

Metallurgy Division
Materials Science and Engineering Laboratory
National Institute of Standards and Technology
Technology Administration, US Dept. of Commerce
Gaithersburg, MD 20899

Abstract

Stress corrosion cracks typically nucleate at a stress concentration in the surface and propagate away from the surface on a plane perpendicular to the applied stress. While this is a good macroscopic description of crack propagation, on a microscopic scale, crack tips regularly deviate from this ideal orientation due to deviations in the preferred microstructural paths for crack propagation and microstructural obstacles. These crack path deviations can be influenced by grain boundary size, shape, and crystallographic texture and may or may not have a significant influence on the accuracy of crack propagation rate measurements or the predictions of propagation rate models. This paper examines the effects that crack path deviations can have on measuring and modeling stress corrosion crack propagation by developing a technique for quantifying these deviations and estimating the difference between the measured and the true rate of crack tip propagation.

Published in "Hydrogen Effects on Material Behavior and Corrosion Deformation Interactions," N. R. Moody, A. W. Thompson, R. E. Ricker, G. W. Was and R. H. Jones, edts., TMS (The Minerals, Metals, and Materials Society), Warrendale, PA (2003) pp. 629-638.

Introduction

Most research into stress corrosion cracking (SCC) uses crack measurement tools and stress intensity calculations that assume crack propagation in a fixed direction on a flat plane with a straight line crack front as illustrated in Figure 1(a). For cracks propagating in this "ideal" manner, the local mode I stress intensity at every point along the crack front, $k_I(z)$, is a maximum equal to the nominal (macroscopic) stress intensity (K_I) calculated for the applied load while the mode II and mode III stress intensities are zero. As illustrated in figure 1(b), real cracks do not propagate in this manner and cracks frequently deviate from the ideal orientation due to the influence of the microstructure or interactions between the microstructure, the applied load, and the environment. Examination of the literature indicates that frequency and magnitude deviations in crack propagation are influenced by alloy composition, grain size, texture, precipitate size and distribution, loading conditions (geometry, strain rates, waveforms, and transients) and environment (1-4).

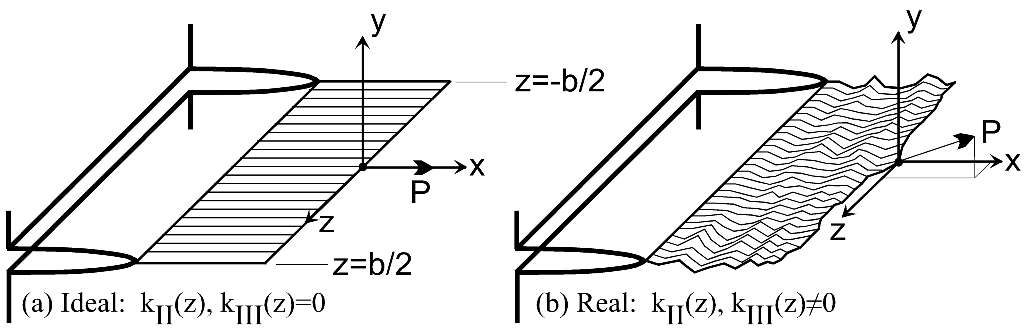

Figure 1. Schematics of (a) the ideal mode I crack propagation assumed for most studies and (b) real crack propagation where deviations from ideal behavior occur frequently.

When cracks deviate from the ideal propagation orientation, $k_I(z)$ will be reduced where deviations occur and the magnitude of these reductions will be related to the deviation between the direction of actual propagation, identified by the propagation vector (P) in figure 1, and the ideal direction of mode I crack propagation (the X-direction). Deviations out of the ideal, mode I, plane of crack propagation will increase the mode II component at the crack tip eventually turning the crack back toward the ideal mode I orientation where $k_{II}(z)=0$ (5). Similarly, deviations in the propagation direction that are in the ideal mode I plane of crack propagation (the XZ plane in Figure 1) will increase the local mode III component at the point of the deviation which will tend to turn the crack front back to the ideal mode I orientation where $k_{III}(z)=0$. Therefore, it is reasonable to assume that these deviations in the direction of crack propagation will be distributed in some regular manner about the ideal orientation with a frequency and magnitude that are determined by the material and the microstructure, as well as the environmental and loading conditions, the distribution of which is reproducible and predictable even if the exact behavior of any point along the crack front is not predictable.

Deviations from the ideal plane and direction of crack propagation will increase the distance a crack must propagate to cause failure (effectively decreasing the rate of crack propagation) and increasing the surface area generated by the fracture. Deviations in the crack front from the straight line configuration assumed by nominal (macroscopic) stress intensity calculations will lower the local crack tip stress intensities along the crack front, $k_I(z)$, while increasing the length of the crack front and the total volume of plastic zone deforming to support the applied load. Both slowing crack propagation and lowering local stress intensities will help a material resist failure. The use of microstructurally induced deviations in crack path to retard or even prevent SCC is not a new concept and the influence of orientation on SCC susceptibility and crack propagation rates in wrought products has long been attributed to this effect, as illustrated for an Al alloy in Figure 2 (6-9). Similarly, texture has been used to avoid SCC or hydrogen embrittlement in materials where there is a well known and preferred microstructural path for crack propagation such as Zr and Ti alloys (10) and failures in service have been attributed to loss of the resistant microstructure or texture as a result of welding. The objective of this research is develop a relatively simple scheme for quantification of the influence of deviations in crack path that enables analysis of the influence of microstructure on the measured rate of crack propagation and susceptibility to SCC.

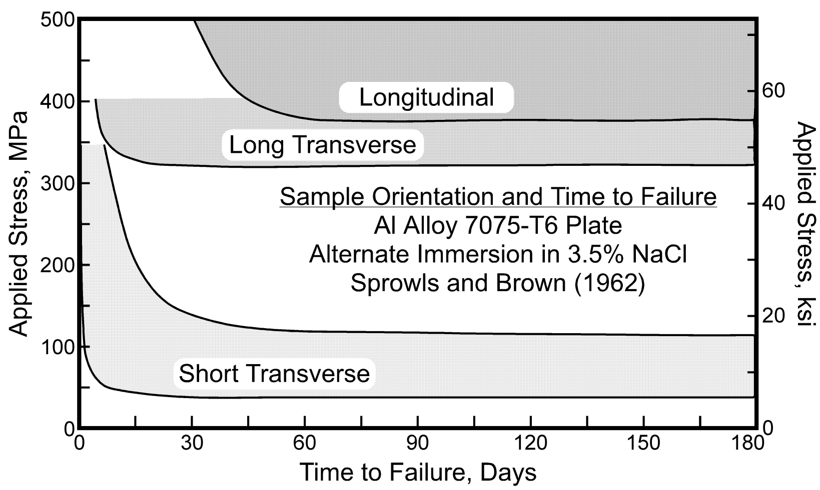

Figure 2. The influence of sample orientation on the intergranular SCC of an Al alloy where changing sample orientation alters the availability of favorably oriented crack paths (adapted from refs. (8,9)).

Quantification of Deviations

Since it is the deviations from the ideal mode I crack configuration that are of primary concern, the analysis can be simplified by reducing the fracture morphology to a distribution of deviations from the ideal orientation for crack propagation as illustrated in Figure 3. This figure shows a top and side view schematic of a typical crack propagation sample with crack profiles and the X,Y, and Z coordinates identified. For this coordinate system, the X-direction is the ideal direction for mode I crack propagation. Assuming that the true direction of crack propagation at some point z along the crack front, P(z), is perpendicular to the crack front line tangent, t(z), and in the plane of the fracture surface as shown in Figure 3(c), then the propagation direction is the vector product of the crack front line tangent and the normal to the fracture plane, n, and the angle, θ, between this direction and X-direction is the deviation from the ideal mode I direction. However, it is difficult to determine θ experimentally from crack side profiles or crack front marks in fractographs, which reveal the trace of the propagation direction in the plane of the view as shown in Figures 3(a) and 3(b), but since out-of-plane (mode II) and in-plane (mode III) deviations may effect crack propagation differently, quantifying deviations by distribution of these components was deemed appropriate.

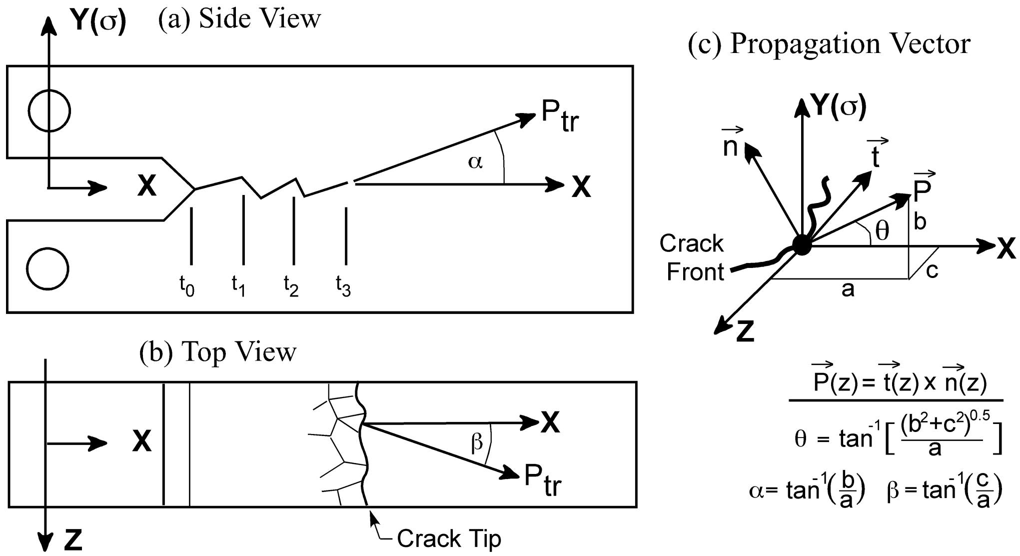

Figure 3. Typical crack propagation sample with coordinates and crack shown in (a) side view (b) top view and (c) at a point, z, along the crack front.

Figures 4 and 5 show two typical SCC crack propagation profiles taken from published literature (2,3). The side view (Y-Z plane) propagation profiles are shown in Figures 4(a) and 5(a). For this analysis, these profiles were traced into a computer and broken into short straight line segments with the out-of-plane propagation angle and distance propagated calculated for each segment. This analysis assumes that the crack propagates at an angle within 90° (±π/2) of the ideal propagation direction. The percent of total measured propagation was determined for each segment and then the segments were sorted to estimate probability density functions (PDFs) with the histograms shown in Figure 4(b) and 5(b). The cumulative distributions for the propagation angles where the ordinate is the fraction of total crack propagation that occurred at propagation angles equal to or less than the abscissa are shown in Figures 4(c) and 5(c).

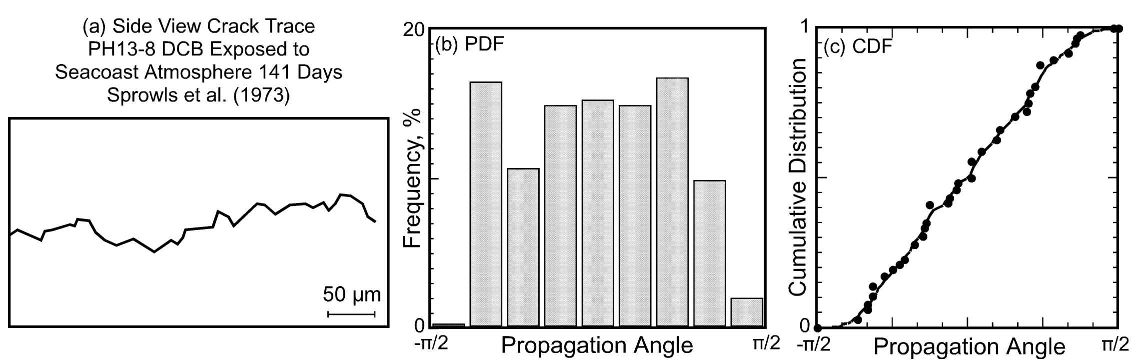

Figure 4. SCC Crack profile on x-y plane (a) with PDF histogram (b) and CDF curve (c) determined for crack.

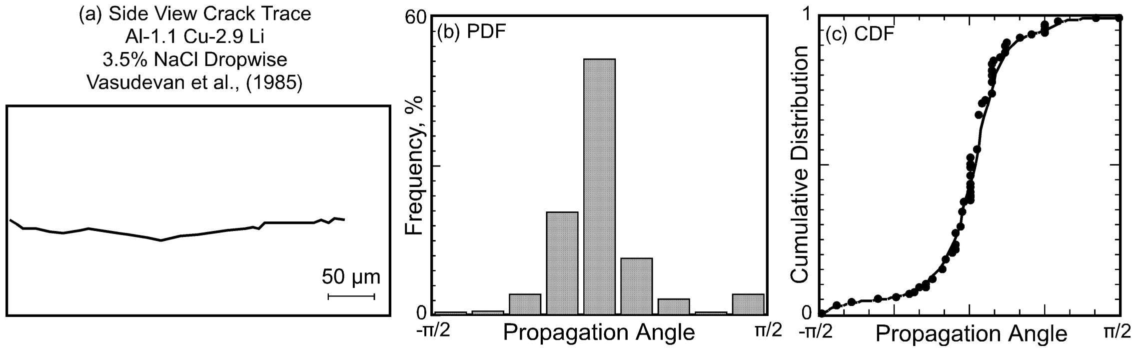

Figure 5. SCC crack profile on x-y plane (a) with PDF histogram (b) and CDF curve (c) determined for crack.

Representation of Deviations

The next issue to be addresses was how to mathematically represent the pattern of deviations in crack path such as those presented in Figures 4 and 5. Since any function can be used as a PDF to represent probabilities and we have assumed that the probability goes to zero at $-\pi/2$ and $\pi/2$ with a maximum at $\alpha=0$, cosine functions of the form

$$\rho(\alpha) = A_n \cos^n(\alpha) \tag{1}$$

where the exponent n defines the dispersion (sharpness or breadth) of the distribution and A_n is the weighting factor are ideal candidates. The weighting factor is determined from the assumption that the sum of all probabilities between $-\pi/2$ and $\pi/2$ is one. A PDF of this form is particularly satisfying since the driving forces returning a crack to the ideal condition (K_I and K_{II}) are a function of the cosine of this angle. Figure 6 shows the PDFs and CDFs for different values of n. By comparing this figure to Figures 4(c) and 5(c) shows that an n of 1 closely fits the results shown in Figure 4(c) and n=8 closely fits the results of Figure 5(c).

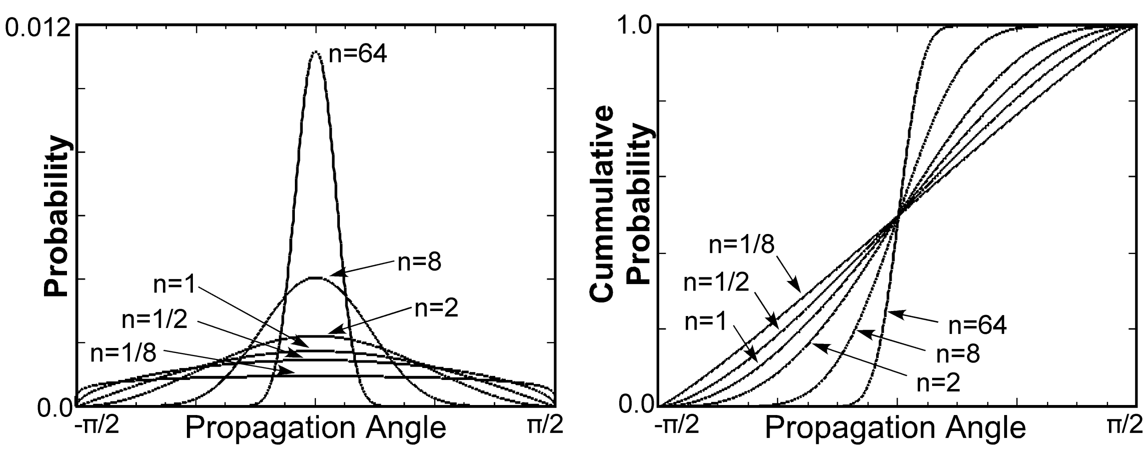

Figure 6. Probability density functions (PDF) and cumulative distribution functions for different values of the dispersion exponent (n).

Influence on Crack Propagation Rates

To estimate the influence of these microstructurally induced deviations from ideal crack propagation on the measured rate of crack propagation, one must first establish the relationship between the true, crack tip, propagation rate (V_{ct}) and the measured propagation rate (V_{meas}). Considering out-of-plane deviations only, this is simply

$$V_{meas} = V_{ct} \cos(\alpha) \tag{2}$$

The expected value for a crack with a pattern of deviations represented by eq. (1) is then

$$\left\langle V_{meas} \right\rangle = \int_{-\pi/2}^{\pi/2} V_{ct} \cos(\alpha) A_n \cos^n(\alpha)\, d\alpha \tag{3}$$

where the expected value is the most likely value to be observed which is also the average value that should be determined for a number of measurements if the sample is large enough to represent the population. The deviations slow the rate of propagation, but since most measurement techniques determine the extent of propagation in a fixed direction over set time intervals, these measurements are averages over the time and distance between the measurement points (ie. the expected value of V_{meas}). Table I shows the suppression ratio (V_{meas}/V_{ct}) for different values of the dispersion parameter n used to quantify the out-of-plane deviations in the propagation angle. For an n of 1, which was found appropriate for representing the results of Figure 4, Table I shows that the out-of-plane deviations alone should reduce the effective crack propagation rate by 27% while for n=8, Figure 5, the reduction is a more modest 6%. This result can be extend to include the in-plane deviations by replacing eq. (2) with a relationship for both angles (α and β) and forming a double integral analogous to eq. (3). On the other hand, one could assume that the measured distributions for the out-of-plane angle (α) are estimates from the trace of the true deviation angle (θ) on the observation plane, and therefore, narrower. Then, the impact of including these deviations can be estimated by examining the influence of proportionately lower values for the dispersion exponent n.

Table I. Estimated average crack propagation rate suppression ratios considering out-of-plane deviations only for different dispersion exponents, n.

n	$\left[\frac{\langle \mathbf{V_{meas}} \rangle}{\mathbf{V_{ct}}}\right]$	$\left[\frac{\mathbf{V_{ct}}}{\langle \mathbf{V_{meas}} \rangle}\right]$
1/8	0.6654	1.5029
1/2	0.7295	1.3708
1	0.7854	1.2732
2	0.8488	1.1781
8	0.9461	1.0570
64	0.9923	1.0077

Influence on Susceptibility to SCC

The ultimate issue is SCC susceptibility. That is, can a microstructure with a built-in set of features that deflect crack propagation from the ideal plane and direction resist crack propagation effectively increasing the load bearing capability of the material and K_{1SCC}. At the crack tip, it will be assumed that the local stress intensity, k_I, is a function of the far-field (macroscopic) stress intensity (K_I) such as

$$k_I = a_{11}(\alpha)K_I \tag{4}$$

in this relationship, K_I is the macroscopic stress intensity normally calculated using flat crack plane and straight line crack front assumptions. The expected value for the local stress intensity is then

$$\left\langle k_I \right\rangle = K_I A_n \int_{-\pi/2}^{\pi/2} a_{11} \cos^n(\alpha) d\alpha \tag{5}$$

Unfortunately, relationships for the influence of in-plane variations in the crack front on local stress intensities are not available in the literature. Therefore, only out-of-plane variations can be considered here. Also, the relationships derived for out-of-plane variations assume a long straight-line crack with a single kink at the end such as that illustrated in Figure 7 (5,11,12). These relationships also assume that the branch is sufficiently long to fully develop the normal plastic zone and are two-dimensional (they assume no change in the third dimension through the sample). For these conditions, Suresh and Shih (12) derived the following limiting cases for a_{11}

$$\text{For}\left(\frac{b}{a}\right) \rightarrow 0 \quad a_{11}(\alpha) = \frac{1}{4}\left[3\cos\left(\frac{\alpha}{2}\right) + \cos\left(\frac{3\alpha}{2}\right)\right] \tag{6}$$

$$\text{For}\left(\frac{b}{a}\right) > \frac{1}{2} \quad a_{11}(\alpha) = \cos^2(\alpha) \tag{7}$$

Taking these relationships for the influence of out-of-plane variations on the local crack tip stress intensity for different values of n yields Table II. By examining this table, it can be seen that deviations in the propagation angle from the ideal assumption serve to lower the expected or average local k increasing the ability of the sample to support the applied load without cracking. That is, if one assumes that there is a critical local stress intensity for SCC and that cracks will only propagate if a significant percentage of the crack front is at or above this stress intensity, then promoting deviations will serve to increase the externally applied (macroscopic) load required to reach this condition.

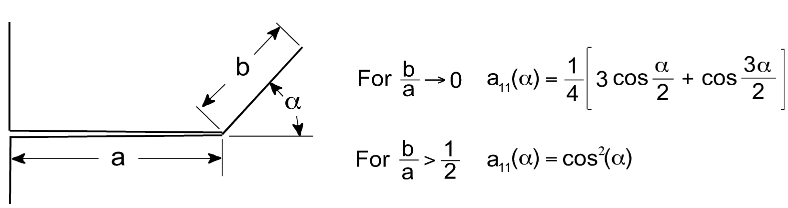

Figure 7. Kink geometry for local, crack tip, stress intensity calculations (12).

Table II. Estimated average crack tip stress intensity suppression factors for different dispersion exponents (n) considering out-of-plane deviation only.

n	**$<k_I>/K_I$ b/a>0.5**	**$<k_I>/K_I$ b/a≈0**
1/8	0.5297	0.7690
1/2	0.6000	0.8112
1	0.6667	0.8485
2	0.7500	0.8917
8	0.9000	0.9603
64	0.9848	0.9943

Discussion

Most methods for the measurement of crack propagation, such as optical crack trace measurements, potential drop, and mechanical compliance, measure the extent of crack propagation in a direction that is fixed in the sample prior to the experiment as illustrated in Figure 3(a). Typically, when large macroscopic deviations from the fixed direction of crack propagation occur, the experiment is declared void and repeated. However, it is the frequency of propagation at large deviation angles and not how far a crack propagates before turning that determines the discrepancy between the effective (measured) crack propagation rate and the true rate of crack tip propagation. On the other hand, stress intensity estimates will be better the closer the macroscopic plane and direction of propagation are to the ideal unless length-dependent roughness corrections can be developed. From a mechanical design standpoint, it is the extent of propagation across the load-bearing member that is the main concern, not the actual distance the crack tip may have propagated to produce this reduction in load bearing capability. From a metallurgical design standpoint, a tool that enables quantification of the influence of microstructural variables on the natural behavior of cracks during propagation will enable more quantitative study of these factors and more thorough use of microstructure to resist SCC. With respect to modeling, this tool should enable better representation of the influence of microstructure both through crack deflection and through other mechanisms because it will enable elimination of ambiguities that crack deflection effects produce. Therefore, this tool should enable better understanding of metallurgical effects on SCC, modelling of SCC, and the design of more SCC resistant microstructures.

The analysis presented in this paper considered only the influence of out-of-plane variations on the measured velocity of crack propagation. However, the influence of in-plane variations on crack propagation rates can be estimated by assuming a broader dispersion constant in Table I or by calculation of suppression ratios with a double integral to include both in-plane and out-of-plane deviation angles. Similarly, only the influence of out-of-plane deviations on the average local crack tip stress intensity was considered. Unlike crack propagation rate measurements, in-plane deviations could not be considered because relationships for the influence of these deviations on the local crack tip stress intensity are not available in the literature. Also, the solutions for out-of-plane deviations assume that the kink is sufficiently long to fully develop the plastic zone and that the kink is uniform through the sample. Clearly, smaller deviations, both in-plane and out-of-plane, will influence the local stress intensity in the direction predicted by the relationships, but the magnitudes of these effects are unclear at this time. Comparing the predictions in Tables I and II with the influence of orientation on the susceptibility of Al alloys to SCC, Figure 2, shows that both indicate a trend in agreement with experiments, but the magnitudes appear insufficient to explain observations. The results of Sprowls and Brown (8,9) indicate that almost an order of magnitude increase in load carrying capability is possible with a change from ST to longitudinal loading and about a order of magnitude decrease in the rate of crack propagation (assuming zero crack initiation time). These results fall short on both, but not so much so that it makes this approach appear invalid. Instead, it appears that more appropriate description of the crack geometry or comparison to more representative crack propagation experiments might yield better information on the magnitude of these effects and the interactions that may need to be included to fully describe crack propagation behavior, unify smooth sample susceptibility and long crack propagation measurements, and enable better prediction of in-service behavior.

Conclusions

A simple method for representing and quantifying the influence of natural, microstructurally induced, distributions from ideal crack propagation was developed. This method quantifies only the distribution of deviations from the normally assumed ideal direction and plane of crack propagation; thereby, simplifying analysis. The influence of distributions of out-of-plane deviation angles on measured crack propagation rates was quantified for distributions in the range of those observed experimentally and found to be significant. Similarly, the influence of these distributions on the average local crack tip stress intensity was evaluated and also found to be significant. Both predict trends with increasing fracture roughness that agree with experimental observations found in the literature, but the predicted magnitudes for these simple distributions and assumptions are less than those frequently observed in experiments.

References

1. M. V. Hyatt and M. O. Speidel, "Stress-Corrosion Cracking of High-Strength Aluminum Alloys," Boeing Commercial Airplane Group, D6-24840, Seattle, WA, (1970).

2. D. O. Sprowls, M. B. Shumaker and J. D. Walsh, "Evaluation of Stress-Corrosion Cracking Susceptibility Using Fracture Mechanics Techniques," Aluminum Company of America, NASA Contract Rpt., NAS 8-21487, Alcoa Center, PA, (1973).

3. A. K. Vasudevan, R. G. Malcolm, W. G. Fricke and R. J. Rioja, "Resistance to Fracture, Fatigue and Stress-Corrosion of Al-Cu-Li-Zr Alloys," ALCOA Laboratories, Tech. Rpt., ONR Cont. No. N00019-80-0569, Alcoa Center, PA, (1985).

4. A. K. Vasudevan and S. Suresh, "Microstructural Effects on Quasi-static Fracture Mech. in Al-Li Alloys: the Role of Crack Geometry," Mater Sci Eng, 72 (1985), 37-49.

5. B. Cotterell and J. R. Rice, "Slightly Curved or Kinked Cracks," Intl J Fract, 16 (2) (1980), 155-169.

6. E. H. Dix, "Acceleration of the Rate of Corrosion by High Constant Stresses," Trans AIME, 137 (1) (1940), 11-40.

7. E. H. Dix, "Al-Zn-Mg Alloys Their Development and Commercial Production," Trans ASM, 42 (1950), 1057-1127.

8. D. O. Sprowls and R. H. Brown, "What Every Engineer Should Know About Stress Corrosion of Aluminum, Part 1," Met Prog, 81 (4) (1962), 79-85.

9. D. O. Sprowls and R. H. Brown, "What Every Engineer Should Know About Stress Corrosion of Aluminum, Part 2," Met Prog, 81 (5) (1962), 77-83.

10. B. Cox, "Environmentally-Induced Cracking of Zirconium Alloys-A Review," J Nucl Mater, 170 (1) (1990), 1-23.

11. B. A. Bilby, G. E. Cardew and I. C. Howard, "Stress Intensity Factors at the Tips of Kinked and Forked Cracks," Proceedings of Fracture 1977, Waterloo, Canada, 3 (1977),

12. S. Suresh and C. F. Shih, "Plastic near-tip Fields for Branched Cracks," Intl J Fract, 30 (1986), 237-259.